3894–3900 Nucleic Acids Research, 1995, Vol. 23, No. 19

Cleavage of double-stranded DNA by 'metalloporphyrin-linker-oligonucleotide' molecules: influence of the linker

Pascal Bigey, Geneviève Pratviel and Bernard Meunier*

Laboratoire de Chimie de Coordination du CNRS, 205 route de Narbonne, 31077 Toulouse cedex, France

Received June 29, 1995; Revised and Accepted August 24, 1995

ABSTRACT

Manganese porphyrin-linker-triple-helix-forming oligonucleotide molecules were prepared and their ability to cleave *in vitro* a double-stranded DNA target present in the HIV-1 genome was studied. The nature of the linker is a determining factor of the cleavage efficiency. Cleavage yields as high as 80% were observed when the linker was a spermine residue and in the absence of a large excess of free spermine known to stabilize triplex structures. The hydrophobic nature of aliphatic diamine linker modified the cleaver–DNA interactions and reduced the efficiency of DNA cleavage.

INTRODUCTION

Modified synthetic oligodeoxynucleotides (ODN) can be considered as new tools in the selective inhibition of gene expression and as potential drugs in anticancer or antiviral chemotherapy (1,2). The target is a mRNA sequence in the antisense approach or a double-stranded DNA sequence in the antigene strategy (2–6). Despite the low melting temperature of a triple helix (T_m values range from 20 to 30°C for ODNs of 16–25 bases compatible with specific sequence recognition, see refs 7–9 for examples), HIV-1 transcription was inhibited by using a triple helix-forming oligonucleotide (TFO) that binds to the transcription initiation site (10) on the polypurine tract (PPT) near U3 sequence or by using a TFO overlapping this PPT (11) on the viral RNA.

Here we report the preparation of 'manganese porphyrin-linker-oligonucleotide' molecules (see Fig. 1 for structures) and their ability to cleave a double-stranded DNA target present on the 5′ side of U3 sequence and also in the *pol* gene of HIV-1 genome. As cleaver moiety we used a tris-methylpyridiniumyl-porphyrinato-manganese(III) motif, Mn-TrisMPyP, because of its ability to perform oxidative DNA breaks when activated by potassium monopersulfate, $KHSO_5$ (for recent articles on the oxidative DNA cleavage involving transition metal complexes, see refs 12–19). The manganese porphyrin entity was linked to the 5′ end of a 16mer TFO via a polyamine, spermine (7) or via various diamines (including ethylenediamine, hexamethylenediamine and dodecamethylenediamine), in order to study the influence of the length and the nature of the linker (see Scheme 1 for structures). High yields of DNA cleavage were obtained when spermine was used as tether in these TFO-cleaver molecules due to the enhanced stabilisation of the triplex by the spermine linker.

MATERIALS AND METHODS

Oligonucleotides: synthesis and functionalization

The two complementary 29mer oligonucleotides (ODN 1 and ODN 2) and the unmodified 16mer TFO used in this study were synthesized by standard solid-phase β-cyanoethylphosphoramidite chemistry on a Cyclone Plus DNA synthesizer from Milligen Biosearch (see Scheme 1 for sequences). Concentrations of single-stranded oligonucleotides were determined by UV titration at 260 nm (20). The 16mer TFO was functionalized at the 5′ position with spermine or diamines (ethylenediamine, hexamethylenediamine or dodecamethylenediamine) as previously described for diamines (21).

For spermine functionalization 50 mg of 1,1′-carbonyldiimidazole (CDI, 300 µmol) were dissolved in 1 ml of anhydrous dioxane. This solution was allowed to pass through a 1 µmol DNA cartridge carrying the oligonucleotide with protected bases and the free 5′-OH (detritylated with dichloroacetic acid) by using two syringes. The activation proceeded for 30 min at room temperature. After this time, the cartridge was washed with dry dioxane (3 × 4 ml). The activated ODN was then allowed to react with a 1 ml solution of spermine [$NH_2(CH_2)_3NH(CH_2)_4NH(CH_2)_3NH_2$, 50 mg, 250 µmol] in a 9/1 dioxane/water mixture, also by using two syringes. The reaction was allowed to proceed for 45 min at room temperature. Then reagents were washed off with dioxane (3 × 4 ml), methanol (3 × 4 ml) and acetonitrile (3 × 4 ml). The cartridge was then argon-dried, opened and the solid support was treated overnight at 55°C with 33% aqueous NH_4OH for cleavage and deprotection. The ammonium hydroxide solution was removed under vacuum. The reaction yield was 90%, as determined by HPLC analysis of the reaction medium (reverse phase Nucleosil C18 column eluted in a gradient mode triethylammonium acetate 0.1 M, pH 6.5/CH_3CN from 15 to 30% of CH_3CN in 40 min at a flow rate of 1 ml/min. Detection was performed at 260 nm. The functionalized 16mer was purified on a 20% denaturing polyacrylamide gel. It should be noted that purification of G-rich oligonucleotides is always complicated by the formation of G-quartets (22,23). About 35 OD (220 nM) of the functionalized 16mer spermine-TFO were recovered from a 1 µmol cartridge.

* To whom correspondence should be addressed

Conjugates **1** to **5**

Mn^{III} TrisMPyP-O-$(CH_2)_m$-CO-NH-$(CH_2)_n$-NH-CO-O-TTTTCTTTTGGGGGGT-$^{3'}$OH

length

conjugate	length*	m	n
1	8	1	2
2	11	4	2
3	15	4	6
4	21	4	12
5	28	11	12

Mn^{III}TrisMPyP- =

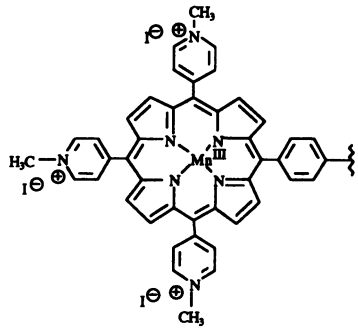

Conjugate **6** (length* = 21)

Mn^{III} TrisMPyP-O-$(CH_2)_4$-CO-NH-$(CH_2)_3$-NH-$(CH_2)_4$-NH-$(CH_2)_3$-NH-CO-O-TTTTCTTTTGGGGGGT-$^{3'}$OH

Spermine

Figure 1. Structures of Mn(TrisMPyP-diamino-5′-TFO) **1–5** and structure of Mn(TrisMPyP-spermine-5′-TFO) **6**. *Length is defined as the number of bonds between the O-atom of the metalloporphryrin-phenexo and the 5′-O of the oligonucleotide.

Preparation of oligonucleotide–metalloporphyrin conjugates

The metalloporphyrin precursors used in this work were prepared according to ref. 24. Conjugates **1–5** were prepared according to published methods (25) and purified by denaturing 20% polyacrylamide gel electrophoresis. Conjugate **6** was synthesized using the following procedure: 1 mg of MnTrisMPyP-COOH (m = 4, 0.8 μmol), 1.7 mg of dicyclohexylcarbodiimide (DCC, 8 μmol) and 1.3 mg of 2-mercaptothiazoline (11 μmol) were dissolved in 50 μl of anhydrous DMSO. The activation was allowed to proceed for 20 min at room temperature. The excess of DCC was then eliminated by addition of 10 μl of 20 mM MOPS buffer [sodium salt of 3-(*N*-morpholino)propanesulfonic acid, pH = 7.5]. The solution of the activated ester was added to the functionalized 16-mer spermine-TFO (7 OD units, 45 nmol) dissolved in 150 μl of buffer (20 mM MOPS, pH 7.5). The reaction was allowed to proceed for 30 min at room temperature. One milliliter of cold ethanol was then added and the mixture was allowed to precipitate overnight at –20°C. After centrifugation, the supernatant was withdrawn. The precipitate was dissolved in 50 μl of water and conjugate **6** was purified on a 20% denaturing polyacrylamide gel. Yield (measured by UV absorbance at 260 nm) after purification and desalting was ~60% for the hybrid molecule with respect to the 5′-spermine-ODN. Purified conjugate **6** showed the two typical absorbance at λ = 468 nm for the metalloporphyrin moiety and λ = 260 nm for the oligonucleotide part (see ref. 25).

Triple helix formation and melting temperatures

Triplex formation was followed by UV spectroscopy. Melting curves were obtained with a diode array HP 8452 spectrophotometer equipped with a Peltier temperature controller (heating increments of 1°C from 10 to 35°C, 3°C from 35 to 56°C and 2°C from 56 to 90°C). The temperature of the solution was stabilised for 7 min at each step before measurement. One centimeter pathlength cuvettes were used for data collection. The duplex absorbance was measured by using a solution containing 1.9 μM of target duplex dissolved in 1.2 ml of buffer (25 mM Tris–HCl, pH 7.1, 100 mM NaCl, 10 mM $MgCl_2$). The triplex absorbance was measured by using a solution containing 1.9 μM of target duplex and 1.9 μM of conjugate dissolved in 1.2 ml of the buffer described above. The melting point of the triplex was determined from the curve corresponding to the difference between triplex absorbance and duplex absorbance plotted versus temperature.

Cleavage experiments

The 29mer target duplex ODN 1·ODN 2 was labelled at the 5′-end of the pyrimidine rich strand ODN 2 by reaction with [γ-^{32}P]ATP and T_4 polynucleotide kinase. In cleavage experiments triplex formation was achieved by incubation of the duplex ODN 1·ODN 2 (10 nM) and the conjugate (1–100 nM) in a 10 μl volume containing 25 mM Tris–HCl (pH 7.1), 100 mM NaCl and 10 mM $MgCl_2$. The hybridization mixture was heated at 90°C for 5 min and slowly cooled to room temperature within 4 h and stored at 4°C overnight to complete the hybridization process. Controls with the free Mn-TrisMPyP-COOH (with m = 4) were performed by incubating the duplex ODN 1.ODN 2 with this metalloporphyrin in the same conditions used in triplex experiments.

For cleaving experiments, 2 μl of a 6 mM $KHSO_5$ solution were added at room temperature (22°C) to 10 μl of hybridization mixture and the reaction was allowed to proceed for 1 h. The reaction was stopped by addition of 1 μl of 1 M HEPES buffer (pH 8). Samples were then diluted with 1 μl of yeast tRNA (10 mg/ml), 100 μl of 0.3 M sodium acetate (pH 5.2) and precipitated with 300 μl of ethanol. The pellet was finally rinsed with 70% aqueous ethanol and lyophilised. Fragments of DNA were

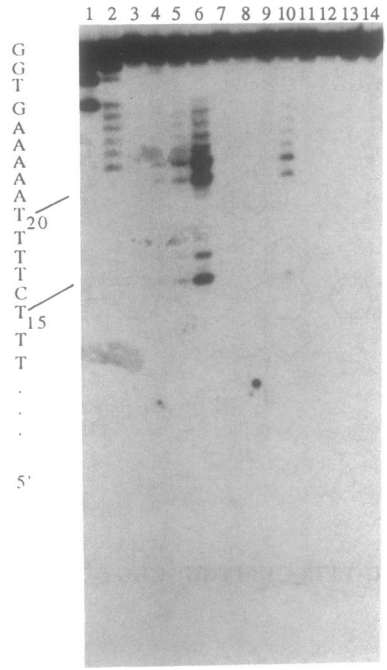

Figure 2. Influence of the length of the linker on the cleaving efficiency of conjugates **3–5**. Analysis by electrophoresis of the cleavage of the duplex target ODN 1·ODN 2 (ODN 2 is labelled at its 5′-end). The target is 10 nM. Lanes 1 and 2: Maxam–Gilbert, G, A+G. Lanes 3–6: 10 nM, 50 nM, 100 nM and 1 μM of the conjugate **3**, respectively, with 1 mM $KHSO_5$. Lanes 7–10: same concentrations of conjugate **4**, respectively, with 1 mM $KHSO_5$. Lanes 11 to 14: same concentrations of conjugate **5**, respectively, with 1 mM $KHSO_5$. All cleavage reactions were performed at room temperature.

analysed by denaturing 20% polyacrylamide gel electrophoresis (26).

RESULTS

The relative abilities of conjugates **1–6** to cleave DNA were examined (see Fig. 1 for structures of conjugate **1–6**). The Watson–Crick 29mer target duplex ODN 1·ODN 2 contains the polypurine sequence present on the 5′ side of U3 of HIV-1 genome (positions 8626–8641 according to ref. 27). The same 16-purine sequence is also present in the *pol* gene (4331–4346). All these oligonucleotides are shown in Scheme 1.

Thermal stability of the triplexes

The TFO containing a 5-methylcytosine is oriented parallel to the polypurine tract of ODN 1 by Hoogsteen pairing (8). The presence of spermine as linker with two protonable sites within the tether contribute to the stabilisation of the triplex. The melting point of conjugate **6** is 42 ± 2°C, so this triple helix is possible at physiological temperature. The T_m values of conjugates **1–5** are observed at 30 ± 2°C when the spermine linker is replaced by an aliphatic diamine. These latter T_m values are also observed for the 5′-OH TFO or the 5′-aliphatic amine-TFO.

5′-X-TTTTCTTTTGGGGGGT (16-mer, **TFO**)
5′-CCACTTTTTAAAAGAAAAGGGGGGACTGG (29-mer, **ODN 1**)
3′-GGTGAAAAATTTTCTTTTCCCCCCTGACC (29-mer, **ODN 2**)
20 15 1

Scheme 1. C is a 5-methylcytosine and X = metalloporphyrin-linker (see Fig. 1).

DNA cleavage with conjugates 1–5: influence of the length of the linker

When manganese porphyrin-linker–TFO were activated by potassium monopersulfate (see ref. 18 for the reactivity of high-valent manganese-oxo porphyrin complexes with DNA), we previously reported that DNA breaks were observed as individual bands when the linker was spermine (19). When conjugates **1–5** are used, the same pattern of cleavage can be observed. The length of the tether of these conjugates (expressed as the number of bonds between the 5′-oxygen of the TFO and the oxygen of the phenoxy group of the Mn-TrisMPyP) is 8, 11, 15, 21 and 28 bonds, respectively. The highest yield of cleavage was obtained with conjugate **3** (15 bonds), using 100 equivalents of **3** with respect to the target duplex (see Fig. 2, lane 6). DNA breaks were observed on the pyrimidine-rich strand and occur mainly at T_{15}, C_{16}, T_{20} and A_{21}. When the tether length was raised to 21 and 28 bonds (conjugates **4** and **5**, respectively), the cleavage efficiency decreased (see Fig. 2, lanes 10 and 14). Conjugate **4** led only to two cleavage bands (T_{20} and A_{21}). With conjugate **5** (28 bonds), no cleavage was observed. On the other side, when the length was decreased to 11 and 8 bonds (conjugates **2** and **1**, respectively), the efficiency of the cleavage also decreased (see Fig. 3, lanes 6, 9 and 12), mainly at the T_{15} and C_{16} positions.

DNA cleavage with conjugate 6

Influence of the nature of the linker. For conjugates **1–5**, the linker between Mn-TrisMPyP and TFO is aliphatic (see Fig. 1). In conjugate **6**, this linker is a spermine molecule, which was previously reported to stabilize triplex structures (19,28–29) because of its protonable sites. We previously reported DNA cleavage with conjugate **6** (19). However, in this communication, cleavage experiments were conducted in a 25 mM Tris–HCl buffer (pH 7.1) with 100 mM NaCl, 10 mM $MgCl_2$ and 2 mM of free spermine, because the addition of free spermine is a classical method to stabilize triplex formation. In fact, potassium monopersulfate used for the manganese porphyrin activation reacted with the free spermine present in large excess in the reaction mixture, so the cleavage yield dramatically decreased (Fig. 4, compare lanes 3–4 and 7–10). The addition of free spermine was not necessary for the triplex formation. Here we report DNA cleavage without free spermine in solution. As shown in Figure 4, conjugate **6** was much more efficient than conjugate **3** (compare lanes 4 and 6). The cleavage efficiency by conjugate **6** is illustrated on the upper part of Figure 4. Eighty percent of the starting material was cleaved. With conjugate **6**, two new cleavage bands appear at positions T_{17} and T_{19}.

Influence of Na^+, Mg^{2+} and temperature. When the temperature is raised from 4°C to room temperature (22°C), the cleavage

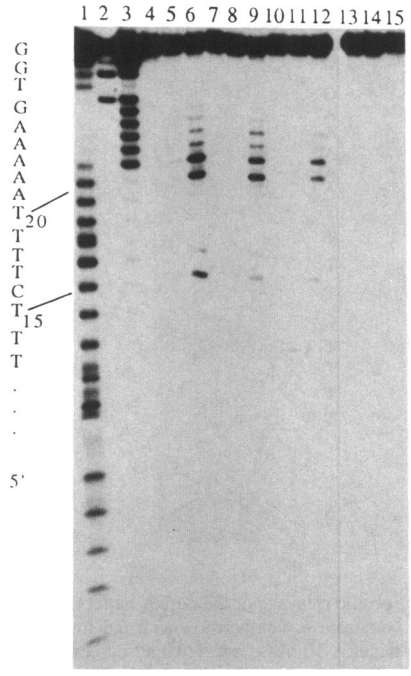

Figure 3. Influence of the length of the linker on the cleaving efficiency of conjugates **1–3**. Analysis by electrophoresis of the cleavage of the duplex target ODN 1·ODN 2 (ODN 2 is labelled at its 5′-end, the target is 10 nM). Lanes 1–3: Maxam–Gilbert, T + C, G, A+G. Lanes 4–6: 10 nM, 100 nM and 1 μM of the conjugate **3**, respectively, with 1 mM $KHSO_5$. Lane 7–9: same concentrations of conjugate **2**, respectively, with 1 mM $KHSO_5$. Lanes 10–12: same concentrations of conjugate **1**, respectively, with 1 mM $KHSO_5$. Lane 13: target duplex only (control). Lane 14: target duplex and 1 μM of the conjugate **3** without $KHSO_5$ (control). Lane 15: target duplex with 1 mM $KHSO_5$ (control). All cleavage reactions were performed at room temperature.

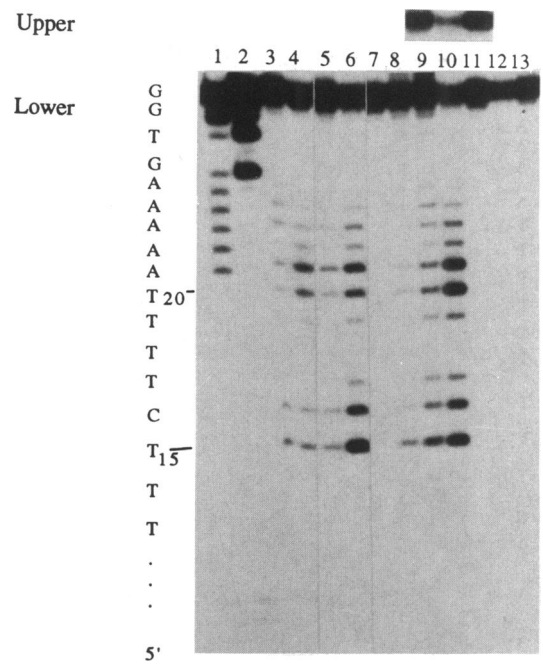

Figure 4. Comparison of the cleavage efficiency of conjugates **3** and **6**. Influence of free spermine and temperature on the cleavage reaction. Analysis by electrophoresis of the cleavage of the duplex target ODN 1·ODN 2 (ODN 2 is labelled at its 5′-end, the target is 10 nM). Lower panel: Lanes 1 and 2: Maxam–Gilbert, A + G, G. Lane 3: 1 μM of the conjugate **3** and 2 mM of free spermine, with 1 mM $KHSO_5$. Lane 4: 1 μM of the conjugate **3**, with 1 mM $KHSO_5$. Lanes 5 and 6: 100 nM and 1 μM of conjugate **6**, respectively, with 1 mM $KHSO_5$. Cleavage reactions were performed at 4 °C for lanes 3–6. Lanes 7 and 8: 100 nM and 1 μM of conjugate **6** and 2 mM of free spermine, respectively, with 1 mM $KHSO_5$. Lanes 9 and 10: 100 nM and 1 μM of conjugate **6**, respectively, with 1 mM $KHSO_5$. Lane 11: target duplex only (control). Lane 12: target duplex and 1 μM of the conjugate **6** without $KHSO_5$ (control). Lane 13: target duplex with 1 mM $KHSO_5$ (control). Cleavage reactions for lanes 7–13 were performed at room temperature. Upper panel: underexposed autoradiogram of the full length material of lanes 9, 10 and 11 of the same experiment.

reaction is more efficient (see Fig. 4, lanes 6 and 10). But at 37 °C, the cleavage efficiency decreased, mainly at T_{20} and A_{21} positions (see Fig. 5, lanes 9 and 10). When the reaction buffer only contains 50 mM instead of 100 mM NaCl, no significant decrease of the cleavage is observed (data not shown).

Divalent cations were reported to be necessary for the formation of purine·purine-pyrimidine triplex (30). In the absence of Mg^{2+} a large decrease in the cleavage yield was observed (Fig. 5, lanes 7 and 8). Mg^{2+} ions seems to be necessary when using a mixed sequence like 5′-TTTTCTTTTGGGGGGT. Controls with free Mn-TrisMPyP-COOH (m = 4) showed that Mg^{2+} had no influence on the cleavage reaction (Fig. 5, compare lanes 14 and 15). In both cases (with and without Mg^{2+}), three individual bands appeared with the same intensity. Therefore, the absence of Mg^{2+} probably inhibited the triplex formation and had no influence on the cleavage reaction.

When a large excess of Herring Testes DNA (HT DNA, 500 nucleotide equivalents with respect to the target) was added after the hybridization reaction (the mixture being allowed to equilibrate overnight before the monopersulfate addition), the cleavage efficiency of **6** slightly decreased (Fig. 6, lane 4). The control experiment with free Mn-TrisMPyP-COOH (m = 4) showed the classical cleavage bands expected for a free metalloporphyrin at positions C_{16}, A_{20} and T_{21} (26). But these bands disappeared when excess HT DNA was added in the reaction mixture (Fig. 6, lane 5).

DISCUSSION

One possible strategy to obtain an irreversible complete inhibition of the expression of integrated double-stranded DNA of HIV is to create oxidative damage on the retroviral genome by using TFO modified with a cleaver. In this case, the chemical yield of this reaction is a crucial point. When using an EDTA-Fe cleaver, the chemical yield for the oxidative cleavage of double-stranded DNA with a third strand equipped with this cleaver is only 15–25% (31).

To find the optimal conditions for obtaining high DNA cleavage efficiency with Mn-TrisMPyP–TFO, we examined the effect of the length and the kind of the linker between the triplex-forming oligonucleotide and the metalloporphyrin. The influences of ionic strength and temperature were also examined.

When the linker is an aliphatic diamine (i.e. ethylenediamine, hexamethylenediamine or dodecamethylenediamine), varying the length caused dramatic changes in the cleavage efficiency. The highest yield was obtained with conjugate **3**, which length is 15 bonds (see Figs 2 and 3). When the length is reduced to 11 or 8 bonds, DNA cleavage becomes lower (Fig. 3). With a short length,

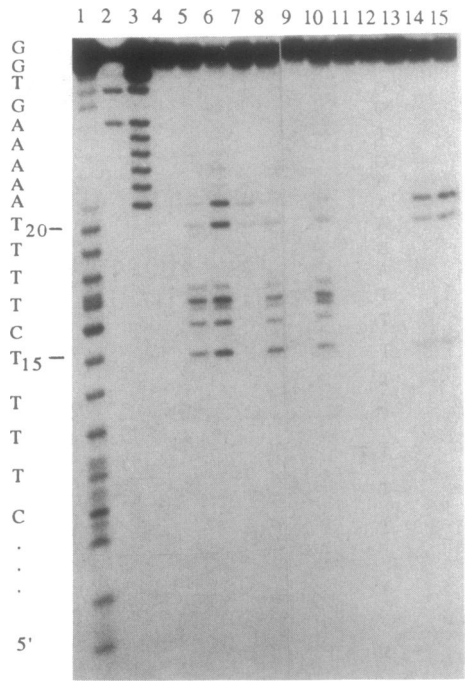

Figure 5. Analysis by electrophoresis of the cleavage of the duplex target ODN 1·ODN 2 by the triplex-forming conjugate **6**. The target is 10nM. Lanes 1–3: Maxam–Gilbert, T + C, G, A + G. Lanes 4–6: 10nM, 100 nM and 1μM of the conjugate **6**, respectively, with 1 mM $KHSO_5$. Lane 7 and 8: 100 nM and 1μM of the conjugate **6**, in a buffer containing 25mM Tris-HCl, pH7.1, 100 mM NaCl and no Mg^{2+}, respectively, with 1 mM $KHSO_5$. Lanes 9 and 10: 100 mM and 1μM of conjugate **6**, respectively, with 1 mM $KHSO_5$, but cleavage reactions were performed at 37°C. Lane 11: target duplex only (control). Lane 12: target duplex and 1μM of the conjugate **6** without $KHSO_5$ (control). Lane 13: target duplex with 1 mM $KHSO_5$ (control). Lane 14: target duplex and 1μM of Mn-TrisMPyP-COOH (m=4), with 1 mM KHSO5, in a buffer containing Tris-HCl 25 mM, pH 7.1, 100 mM, no Mg2+ (control). All cleavage reactions were performed at room temperature, except for lanes 9 and 10 (37°C)

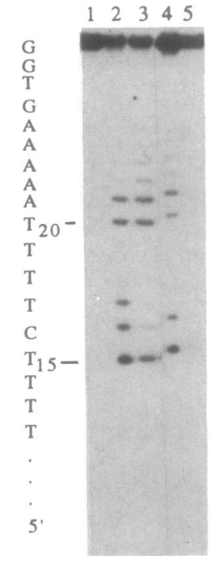

Figure 6. Sequence specific cleavage of the duplex target ODN 1·ODN 2 by the triplex-forming conjugate **6**: comparision with the free Mn-TrisMPyP-COOH (m=4). The target is 10 nM. Lane 1: target duplex and 1μM of the conjugate **6** without $KHSO_5$ (control). Lane 2: 1μM of the conjugate **6** with 1μM $KHSO_5$. Lane 3: target duplex and 1μM of Mn-TrisMPyP-COOH (m=4), with 1mM $KHSO_5$. Lane 4: 1μM of Mn-TrisMPyP-COOH (m=4) and large excess of HT DNA (500 eq.), with 1 mM $KHSO_5$. All cleavage reactions were performed at room temperature.

the metalloporphyrin moiety should stay in the major groove of the target and should be able to cleave by hydroxylation of sugar C-H bonds available within the major groove (H_S2', H3′ and H_R5', see ref. 32) or base oxidation. However, and particularly with conjugate **1**, the cleavage is more specific near the triplex-to-duplex junction (Fig. 3, lane 12) than with conjugate **3**. When the linker length increased, cleavage efficiency decreased (Fig. 2). No cleavage product was observed with conjugate **5** (28 bonds), this might be due to too strong hydrophobic repulsions of the aliphatic linker with DNA. We previously reported that conjugates **3–5** cleaved a single-stranded DNA target with the same efficiency (33), so the hydrophobic nature of the aliphatic diamine linker did not influence the DNA cleavage in the antisense strategy. The data obtained with conjugates **3** and **5** pointed out this factor, important in the antigene approach, negligible in the antisense strategy. When the linker between the TFO and the metalloporphyrin is a spermine molecule, these hydrophobic repulsions are suppressed and replaced by favorable electrostatic interactions because of the two protonable sites of spermine. Though the length of conjugate **6** is 21 bonds (equal to that of conjugate **4**), its cleavage efficiency is much higher (Fig. 4). Spermine linked to oligonucleotides is known to stabilize triple helical complexes (28).

The influence of conjugate **6** concentration was also examined. G-rich oligonucleotides are known to form quadruplex structures (34,35). These structures are stabilized by monocations, particularly with K^+, Rb^+ and Na^+. Formation of quadruplex structure competes with triple helix formation (36). When the concentration of **6** was raised to 10 μM, cleavage efficiency was reduced (data not shown), probably due to G-quartet formation. The maximum cleavage yield was obtained with 1 μM concentration of **6** (Fig. 4). Reducing the Na^+ concentration should reduce the quadruplex formation (36). When Na^+ concentration was 50 mM instead of 100 mM, no significant difference was observed for the cleavage efficiency (data not shown).

Free spermine in solution is known to stabilize triplex structures, and is often required for triplex formation (37). In our case, free spermine did not increase the T_m of the triple helices: the melting temperature of conjugate **6** was ~42°C with or without free spermine; the melting temperature of conjugates **1–5** was ~30°C with or without free spermine. Furthermore, spermine is oxidized by $KHSO_5$, which caused a dramatic decrease of the cleavage efficiency (Fig. 4, lanes 7 and 8).

When a purine-rich TFO is used for triple helix formation, a divalent cation such as Mg^{2+} is necessary (4,30). When we used a Tris–HCl 25 mM, pH 7.1, 100 mM NaCl, buffer containing no Mg^{2+}, we observed a large decrease in the cleavage efficiency of conjugate **6** (Fig. 5, lanes 7 and 8). This is probably due to an inhibition of triple helix formation, and is in agreement with the results previously reported (4,30). No influence of Mg^{2+} was observed on the cleavage yield in the control experiment with free Mn-TrisMPyP-COOH (m = 4 ; Fig. 5, lanes 14 and 15). This shows that Mg^{2+} is really necessary to the triplex formation and that conjugate **6** mediated sequence specific cleavage of the target duplex DNA through the formation of a triple helix. Another

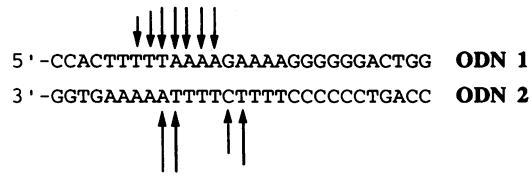

Scheme 2. Pattern of cleavage by conjugate **3** on the duplex target ODN 1-ODN 2. Arrows are proportional to DNA breaks.

experiment was carried out to show that the cleavage of conjugate **6** was triple-helix mediated: the addition of an excess of random HT DNA in the reaction mixture totally displaced the reactivity of the Mn-TrisMPyP-COOH (m = 4) onto the non-labelled random DNA while the conjugate **6** stayed hybridized and cleaved its specific target sequence.

The addition of an excess of HT DNA (500 nucleotide equivalents with respect to the target duplex) after the hybrization reaction slightly reduced cleavage yield, but the cleavage is still sequence-specific (Fig. 6, lanes 2 and 4). The same excess of HT DNA in a mixture containing the target duplex and the free Mn-TrisMPyP-COOH (m = 4) precursor completely inhibited the cleavage reaction (Fig. 6, lanes 3 and 5).

Previous examples of triple-helix-directed cleavage of DNA resulted in efficiencies generally <25% (3,38–40), except with a copper-phenanthroline-oligonucleotide molecule for which a 70% yield has been recently reported by Shimizu *et al.* (41), with 2 μM of cleaver and 100 nM of target. In our best cleavage conditions (i.e. 25 mM Tris–HCl, pH 7.1, 100 mM NaCl, 10 mM $MgCl_2$), the yield of cleavage with conjugate **6** was 80% with 1 μM of cleaver and 10 nM of target, measured by densitometry (Fig. 4, lane 10, upper). This is one of the best cleavage yield reported in the literature, with a cleaver-TFO in a reaction medium deprived of free spermine. The cleavage is also temperature dependent: the yield is higher when the reaction is carried out at 22°C rather than at 4°C (Fig. 4, lanes 5, 6, 9 and 10). As expected, a decrease of the cleavage efficiency was observed at 37°C (Fig. 5, lanes 9 and 10), near the T_m of the triplex formed with conjugate **6**.

The cleavage is efficient on the pyrimidine-rich strand of the target but on the purine-rich strand (i.e. ODN 1) it is weaker (data not shown). Scheme 2 describes the pattern of cleavage that was observed on both strands by using conjugate **3**.

The cleavage sites revealed an asymmetric strand distribution. They are shifted to the 5′-end, indicating that the oxidative reaction occured in the major groove. This is consistent with the fact that conjugate **3** hybridized by triple helix formation and positioned the reactive entity in the major groove whereas the free Mn-TrisMPyP-COOH (m = 4) motif probably cleaved double-stranded DNA by interaction in the minor groove as previously observed for its tetracationic analogue Mn-TMPyP (26). We are currently working on the detailed mechanism of the cleavage reaction.

CONCLUSION

In conclusion, the cleavage of duplex DNA by Mn-TrisMPyP-TFO molecules was examined. The results showed that the linker between the metalloporphyrin and the TFO is of great importance on the cleavage efficiency. If the linker is a long aliphatic chain, no efficient cleavage was observed. The origin of the low cleavage efficiency of conjugates **4** and **5** is considered to be due to strong hydrophobic repulsions. These repulsions are supressed when the linker is a spermine molecule, containing two protonable sites. In this case, the yield of the cleavage reaction was 80%. It was also shown that free spermine in solution is not necessary for the formation of triplex, when the TFO is a G-rich oligonucleotide. Our results demonstrate that highly efficient cleavage of a double-stranded DNA target from the HIV-1 genome *in vitro* may be obtained by using a TFO equipped with a chemical cleaver. Such a reaction might be of interest as an approach to treat infected cells and induce irreversible damage on the viral genome.

ACKNOWLEDGEMENTS

PB is indebted for a PhD fellowship from CNRS and Région Midi-Pyrénées. This work was supported by ANRS (French agency for research on AIDS), ARC (Association pour la Recherche contre le Cancer, Villejuif) and CNRS. Dr Martine Defais (CNRS-LPTF, Toulouse) is acknowledged for making possible experiments with labelled oligonucleotides.

REFERENCES

1 Cohen, J.S. (1989) *Oligodeoxynucleotides, Antisense Inhibitors of Gene Expression.* Macmillan Press, London.
2 Wickstrom, E. (1991) *Prospects for Antisense Nucleic Acids Therapy of Cancer and AIDS.* Wiley-Liss, New York.
3 Moser, H. E. and Dervan, P. B. (1987) *Science*, **238**, 645–650.
4 Uhlmann, E. and Peyman, A. (1990) *Chem. Rev.*, **90**, 543–584.
5 Englisch, U. and Gauss, D. H. (1991) *Angew. Chem. Int. Engl. Ed.*, **30**, 613–629.
6 Thuong, N. T. and Hélène, C. (1993) *Angew. Chem. Int. Engl. Ed.*, **32**, 666–690.
7 Kibler-Herzog, L., Kell, B., Zon, G., Shinozuka, K., Mizan, S. and Wilson, W. D. (1990) *Nucleic Acids Res.*, **18**, 3545–35555.
8 Giovannangéli, C., Rougée, M., Garestier, T., Thuong, N. T. and Hélène, C. (1992) *Proc. Natl. Acad. Sci. USA*, **89**, 8631–8635.
9 Huang, C. Y. and Miller, P. S. (1993) *J. Am. Chem. Soc.*, **115**, 10 456–10 457.
10 Shan, W. M., Rossen, R. D., Laughter, A. H., Trial, J., Kessler, D. J., Zendegui, J. G., Hogan, M. E. and Orson, F. M. (1992) *J. Biol. Chem.*, **267**, 5712–5721.
11 Volkmann, S., Jendis, J., Frauendorf, A. and Moelling, K. (1995) *Nucleic Acids Res.*, **23**, 1204–1212.
12 Dervan, P. B. (1986) *Science*, **232**, 464–471.
13 Sigman, D. S., Bruice, T. W., Mazumder, A. and Sutton, C. L. (1993) *Acc. Chem. Res.*, **26**, 98–104.
14 Le Doan, T., Praseuth, D., Perrouault, L., Chassignol, M., Thuong, N. T. and Hélène, C. (1990) *Bioconj. Chem.*, **1**, 108–113.
15 Singleton, S. F. and Dervan, P. B. (1994) *J. Am. Chem. Soc.*, **116**, 10 376–10 382.
16 Pitié, M., Casas, C., Lacey, C. J., Pratviel, G., Bernadou, J. and Meunier, B. (1993) *Angew. Chem. Int. Engl. Ed.*, **32**, 557–559.
17 Pratviel, G., Duarte, V., Bernadou, J. and Meunier, B. (1993) *J. Am. Chem. Soc.*, **115**, 7939–7943.
18 Pitié, M., Bernadou, J. and Meunier, B. (1995) *J. Am. Chem. Soc.*, **117**, 2935–2936.
19 Bigey, P., Pratviel, G. and Meunier, B. (1995) *J. Chem. Soc., Chem. Comm.*, 181–182.
20 Fasman,G. (1975) *Handbook of Biochemistry and Molecular Biology-Nucleic Acids*, 3rd. edn, CRC Press, Boca Raton, FL, p. 175.
21 Wachter, L., Jablonski, J. A. and Ramachandran, K. L. (1986) *Nucleic Acids Res.*, **14**, 7985–7994.
22 Sen, D. and Gilbert, W. (1990) *Nature*, **344**, 410–414.
23 Marsh, T. C. and Henderson, E. (1994) *Biochemistry*, **33**, 10 718–10 724.
24 Casas, C., Saint-Jalmes, B., Loup, C., Lacey, C. J. and Meunier, B. (1993) *J. Org. Chem.*, **58**, 2913–2917.
25 Casas, C., Lacey, C. J. and Meunier, B. (1993) *Bioconj. Chem.*, **4**, 366–371.
26 Pitié, M., Pratviel, G., Bernadou, J. and Meunier, B. (1992) *Proc. Natl Acad. Sci. USA*, **89**, 3967–3971.

27 Wain-Hobson, S., Sonigo, P., Danos, O., Cole, S. and Alizon, M. (1985) *Cell*, **40**, 9–17.
28 Tung, C. H., Breslauer, K. J. and Stein, S. (1993) *Nucleic Acids Res.*, **21**, 5489–5494.
29 Thomas, T. and Thomas, T. J. (1993) *Biochemistry*, **32**, 14 068–14 074.
30 Beal, P. A. and Dervan, P. B. (1991) *Science*, **251**, 1360–1363.
31 Dervan, P. B. (1992) *Nature*, **359**, 87–88.
32 Pratviel, G., Bernadou, J. and Meunier, B. (1995) *Angew. Chem. Int. Ed. Eng.*, **34**, 746–769.
33 Pratviel, G., Bigey, P., Bernadou, J. and Meunier, B. (1995) In Sarkar, B. (ed.) *Metals and Genetics*. Marcel Dekker Inc., New York, pp. 153–171.
34 Sen, D. and Gilbert, W. (1992) *Biochemistry*, **31**, 65–70.
35 Fang, G. and Cech, T. R. (1993) *Biochemistry*, **32**, 11 646–11 657.
36 Olivas, W. M. and Maher III, L. J. (1995) *Biochemistry*, **34**, 278–284.
37 Singleton, S. F. and Dervan, P. B. (1993) *Biochemistry*, **32**, 13 171–13 179.
38 Strobel, S. A., Moser, H. E. and Dervan, P. B. (1988) *J. Am. Chem. Soc.*, **110**, 7927–7929.
39 Perrouault, L., Asseline, U., Rivalle, C., Thuong, N. T. , Bisagni, E., Giovannangeli, C., Le Doan, T. L. and Hélène, C. (1990) *Nature*, **344**, 348–360.
40 Praseuth, D., Perrouault, L., Le Doan, T. L., Chassignol, M., Thuong, N. T. and Hélène, C. (1988) *Proc. Natl. Acad. Soc. USA*, **85**, 1349–1353.
41 Shimizu, M., Inoue, H. and Ohtsuka, E. (1994) *Biochemistry*, **33**, 606–613.